Check for updates

Metal–organic framework-based separation columns: fundamental study for molecular recognition and potential for separation of linear polymers with close terminal structures†

Keigo Matsubara,[a] Yoshiyuki Watabe,[b,c] Sayaka Konishi-Yamada,[b] Nobuhiko Hosono, [ID] [d] Takashi Uemura [ID] [d] and Takuya Kubo [ID] *[a,b]

We report stationary phases using metal–organic frameworks (MOFs) composed of metal ions and organic ligands in HPLC. We mainly applied $[Zn_2(1,4\text{-}ndc)_2ted]_n$ (ZnJAST4) (ndc: naphthalenedicarboxylate, ted: triethylenediamine) as the stationary phase. To inspect how metal ions and organic ligands affect retention behavior, three different types of MOF, $[Cu_2(1,4\text{-}ndc)_2ted]_n$ (CuJAST4) with zinc ions of ZnJAST4 substituted with copper ions, $[Zn_2(1,4\text{-}bdc)_2ted]_n$ (ZnJAST1) (bdc: benzenedicarboxylate) with the naphthalene of ZnJAST4 substituted with benzene, and ZnJAST4 were packed into columns, and then HPLC using benzene derivatives was conducted to evaluate the recognition ability of these MOFs toward functional groups and shapes of molecules using hexane as the mobile phase. The result revealed that the retention behavior depended on various factors such as halogen bonding, π stacking, molecular shapes, and molecular sizes. Furthermore, to evaluate retention selectivity toward functional groups, HPLC analyses were conducted with a ZnJAST4-packed column with a mobile phase, *N,N*-dimethyl-formamide (DMF), using poly(ethylene glycol) (PEG) derivatives, which have different polar terminal groups, as analytes. The result showed that when the polarity of terminal groups was low, the retention to ZnJAST4 increased.

1. Introduction

In recent years, polymer chemistry has advanced significantly. However, synthetic macromolecules are produced as mixtures having disorganized molecular weight distributions and presenting challenges in this field. Precise syntheses of macromolecules have been enthusiastically examined since living radical polymerization was first reported in the 1990s.[1,2] While precise artificial syntheses of macromolecules with completely uniform chemical compositions and structures have not yet been realized, they are easily generated naturally *in vivo*.

Instead of precise synthesis, separation and purification methods are preferred to obtain such polymers with uniform structures. Although methods including distillation, recrystallization, and extraction are used for the purification of low-molecular weight compounds, these are not applicable to the precise separation of macromolecules. If the chemical composition and structure of individual polymer chains are close, isolation of the specific polymer component from the mixture becomes impractical since slight structural differences hardly affect overall polymer properties.

Against this background, one recent study proposed that metal–organic frameworks (MOFs) could serve as precise molecular recognition sites for polymers.[3] MOFs are coordination polymers composed of metal ions and organic ligands, and they exhibit tunable properties: both pore size and internal chemical structures can be freely designed by varying the combination of metal ions and organic ligands, providing advantages over existing porous materials.[4–6] Because of these features, MOFs have attracted great interest for applications such as gas storage and separation,[7–9] catalysis[10–12] and sensing.[13–15] In addition, MOFs have been employed in optical analysis of gaseous and liquid molecules.[16] Recent studies have revealed that linear polymers, such as poly(ethylene glycol)s (PEGs), linear alkanes, and polythiophenes, can be spontaneously introduced into the pores of MOFs.[17]

[a] Graduate School of Engineering, Kyoto University, Katsura, Nishikyo-ku, Kyoto 615-8510, Japan. E-mail: tkubo@kpu.ac.jp; Tel: +81-75-703-5629
[b] Graduate School of Life and Environmental Science, Kyoto Prefectural University, 1-5 Shimogamo Hangi-cho, Sakyo-ku, Kyoto 606-8522, Japan
[c] Research Center, Shimadzu General Service, Inc, 1, Nishinokyo, Kuwabara-cho, Nakagyo-ku, Kyoto 604-8511, Japan
[d] Department of Applied Chemistry, Graduate School of Engineering, The University of Tokyo, Tokyo 113-8654, Japan
†Electronic supplementary information (ESI) available. See DOI: https://doi.org/10.1039/d5an00548e

Since the study reporting that poly(ethylene glycol)s (PEGs) can be embedded within MOF pores, MOFs have become promising candidates as separation media for polymers. To date, it has been reported that by tuning the size of MOF pores, size exclusion-based sorting of polymers is possible, enabling effective separation of terminal-functionalized polymers.[18–20]

According to these studies, applications of MOFs as separation media in the liquid phase have drawn increasing attention. Some research studies have highlighted liquid chromatography (LC)-based separation techniques for PEGs and their derivatives with various terminal functional groups.[18,21] Notably, HPLC separations[22] using MOF-modified monolith capillary columns have demonstrated superior separation efficiency compared to traditional MOF crystal-particle columns,[23] which are clearly inferior relative to conventional HPLC phases.

In this study, we investigate the molecular recognition capabilities of MOFs as stationary phases in liquid-phase separation and attempt to improve the separation efficiency of MOF columns.

2. Materials and methods

2.1 Synthesis of MOFs and their column packing

To examine molecular recognition when a MOF is applied to the stationary phase in HPLC, two types of MOF besides ZnJAST4, CuJAST4, and ZnJAST1, were synthesized.[24] After observations using SEM, three types of MOF columns were fabricated by packing them with each MOF (Table 1). MOFs were prepared according to the following procedure. Starting materials (shown in Table 1) were combined in a 100 mL eggplant flask, sonicated for 5 min, and the mixture heated at 120 °C for 48 h. (When the temperature inside the flask had reached around 120 °C, it was sealed and heated.) After heating, the product was washed with DMF and dried under vacuum. The amount obtained of all prepared MOFs was more than 3 g. A sample of each MOF was observed using SEM, and then the MOFs (about 500 mg) were wet-packed into 100 mm × 2.0 mm i.d. columns using DMF as the slurry solvent. The wet packing was implemented under the following pressure conditions: 0–5 min at 200 kgf cm^{-2}, then 5–15 min at 500 kgf cm^{-2}.

2.2 HPLC evaluations with MOF packed columns

Employing the column fabricated as described in section 2.1, the retention behavior in hexane as the mobile phase was analyzed using monosubstituted benzenes as analytes. The reten-

tion coefficient k was evaluated as elution time of hexane, t_0, and retention time of analyte, t_R, where $k = (t_R - t_0)/t_0$.

The HPLC conditions were: columns, ZnJAST4 (100 mm × 2.0 mm i.d.), CuJAST4 (100 mm × 2.0 mm i.d.), ZnJAST1 (100 mm × 2.0 mm i.d.); mobile phase, hexane; flow rate, 0.2 mL min^{-1} (ZnJAST4, ZnJAAST1), and 0.1 mL min^{-1} (CuJAST4); temperature, 40 °C; injection volume. 5 μL; detection, UV (254 nm).

2.3 Elution behavior of PEGs with etherified termini in the ZnJAST4 column

The elution behavior of PEG ethers bearing different alkyl chain lengths was investigated using the ZnJAST4 column and N,N-dimethylformamide (DMF) as the mobile phase. The analytes included MeO-PEG-OH (M_n = 2000) and monoetherified derivatives (mPEG-OR) synthesized from MeO-PEG-OH (M_n = 2000). The elution behavior of PEG ethers bearing different alkyl chain lengths was investigated using the ZnJAST4 column and N,N-dimethylformamide (DMF) as the mobile phase. The HPLC conditions were follows: column, ZnJAST4 packed column; injection volume of analytes, 5 μL; measurement temperature, 25, 40, 60 °C; flow rate, 0.2 mL min^{-1}; detector, evaporate light scattering detector for HPLC. The detailed procedures are described in the ESI (Scheme S1 and Table S1†).[17]

2.4 Elution behavior of PEGs with esterified termini in the ZnJAST4 column

Analyses were conducted using mPEG-OH and preparatively purified mPEG-OCOBu as analytes in the ZnJAST4 crystal-packed column. HPLC conditions are as follows: column, ZnJAST4 (100 mm × 2.0 mmm i.d.); mobile phase, DMF; flow rate, 0.2 mL min^{-1}; temperature, 40 °C; detection, RI; injection volume of analytes, 10 μL; analytes, mPEG-OH (raw material), mPEG-OCOR (10 mg mL^{-1} each).

3. Results and discussion

3.1 Synthesis of MOFs and their column packing

Fig. 1 shows the SEM images of MOF crystals obtained after synthesis, revealing that the particle size of CuJAST4 was smaller than that of ZnJAST4 and ZnJAST1. After packing them into the HPLC column, the back pressure was measured. Since the back pressure of the CuJAST4 column was higher than that of the others, the flow rate for subsequent evaluations of the

Table 1 The components of the MOFs

	Metal	Acidic ligand	Basic ligand	Solvent
ZnJAST4	Zn(NO$_3$)$_2$·6H$_2$O (3.49 mmol)	1,4-ndcH$_2$ (3.37 mmol)	ted (1.66 mmol)	DMF (40 mL)
CuJAST4	Cu(CH$_3$COO)$_2$·H$_2$O (3.36 mmol)	1,4-ndcH$_2$ (3.39 mmol)	ted (1.71 mmol)	DMF (40 mL)
ZnJAST1	Zn(NO$_3$)$_2$·6H$_2$O (3.36 mmol)	1,4-bdcH$_2$ (3.41 mmol)	ted (1.71 mmol)	DMF (40 mL)

(1,4-ndcH$_2$): 1,4-naphthalenedicarboxylic acid, (1,4-bdcH$_2$): 1,4-benzenedicarboxylic acid, (ted): triethylenediamine.
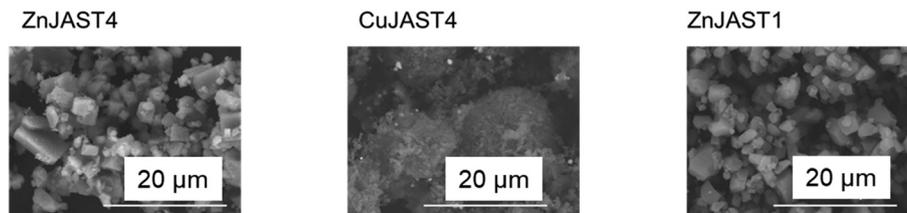
Fig. 1 SEM images of the prepared MOF crystals.

CuJAST4 column was reduced to half compared to the other columns during HPLC.

3.2 Evaluation of the retention behavior of monosubstituted benzenes

Table S2† shows the values of the retention coefficient, k, for monosubstituted benzenes obtained with each column. Strong retention was observed with all columns when using nitrobenzene. This is because carboxyl groups in the ligand of the MOF structures and nitro groups have similar electronic properties and, thus, nitro groups are temporarily captured by the MOF structure.

The elution order of other monosubstituted benzenes exhibited a similar trend on ZnJAST4 and CuJAST4, with halogenated compounds showing increased retention in accordance with the atomic number of the halogen. In contrast, ZnJAST1 displayed a different trend, where bromobenzene exhibited the highest retention. Notably, NO_2-substituted benzene was strongly retained by all the MOFs. Although detailed interaction mechanisms were not evaluated, several factors likely account for observed retention behaviors, including dipole–dipole interactions, halogen bonding, π stacking, and size exclusion effects.[25] In any case, molecular recognition in MOFs may depend more strongly on differences in acidic ligands and pore sizes than on the identity of metallic ions.

3.3 Evaluation of the retention behavior of alkylbenzenes on MOF columns

The values of the retention coefficient, k, of alkylbenzenes with each column were plotted against the carbon number of the alkyl chains (where 0 indicates benzene) as shown in Fig. 2(a). The elution order of ZnJAST4 and CuJAST4 showed similar trends: as the carbon number increased, the retention time became longer. ZnJAST1 exhibited a different trend. The retention coefficient for toluene and ethylbenzene were comparatively large but as the carbon number increased, the retention coefficient became smaller. According to these results, while insertion of the alkyl chain into the pore occurred in the structure of JAST4, the pore size may be too large to stabilize the alkyl chain inside of the pore in the structure of JAST1 in hexane. This assessment corresponds with the sizes of these MOFs, which has been previously reported (Fig. 2(b)).[18,26] Although the length of each MOF structure itself is almost the same in ZnJAST4 and ZnJAST1, due to steric hindrance of the acidic ligands, the pore diameters in these MOF structures are significantly different, at 5.7 Å and 7.5 Å, respectively.

3.4 Evaluation of the retention behavior of disubstituted benzenes

Table 2 shows the values of the retention coefficient, k, of disubstituted benzenes for each column. The analytes with *ortho*-position substituents tend to be retained much more strongly in JAST4. ZnJAST1 showed higher retention toward the analytes with substituents at the *para*-position, but there were exceptions such as dibromobenzene and diiodobenzene. The strong retention of dinitrobenzene was observed with each column where retentions of analytes with substituents at the *ortho* and *para* positions being especially strong. The retention of terphenyl in its *para* configuration was strongest with all of the columns. This may be correlated to how easily molecular
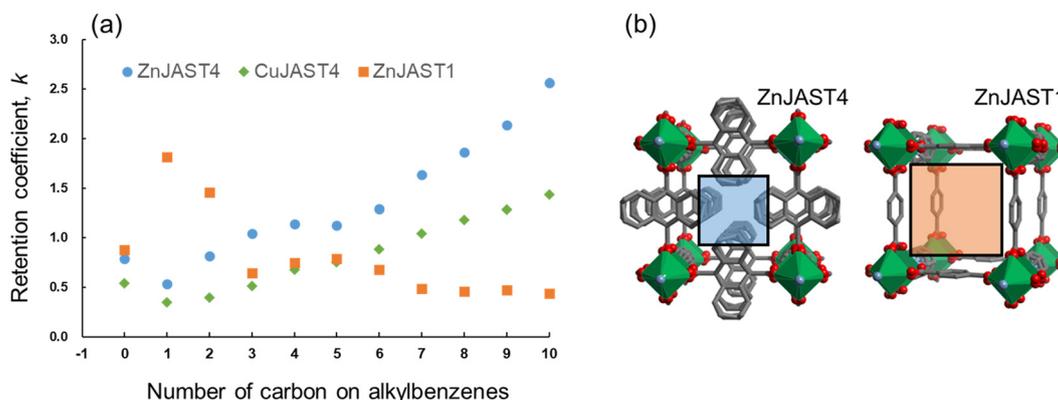

Fig. 2 (a) The retention behavior of alkylbenzenes within the MOF columns, and (b) schematic structures of the ZnJAST4 and ZnJAST1 MOFs.

Table 2 The retention coefficients of disubstituted benzenes in the hexane mobile phase

	Position	ZnJAST4	CuJAST4	ZnJAST1		Position	ZnJAST4	CuJAST4	ZnJAST1
CH_3	ortho	0.35	0.27	4.97	F	ortho	1.14	0.73	0.99
	meta	0.35	0.23	1.65		meta	0.90	0.53	1.12
	para	0.43	0.27	1.79		para	1.76	0.71	4.11
C_2H_5	ortho	0.38	0.22	8.33	Cl	ortho	0.99	0.69	7.43
	meta	0.87	0.38	0.045		meta	0.78	0.48	3.63
	para	1.33	0.63	0.041		para	2.21	0.69	12.7
OCH_3	ortho	3.98	1.58	18.2	Br	ortho	1.35	0.91	17.6
	meta	2.34	1.25	5.90		meta	1.34	0.76	17.6
	para	3.81	1.34	7.98		para	3.43	1.17	11.4
OC_2H_5	ortho	1.96	1.30	2.16	I	ortho	2.17	1.48	21.4
	meta	2.05	1.04	1.19		meta	3.01	1.86	3.46
	para	3.89	1.44	1.24		para	6.13	2.70	3.22
NO_2	ortho	26.4	9.67	109	Phenyl	ortho	0.02	0.03	0.32
	meta	18.2	7.94	53.7		meta	5.09	1.47	0.83
	para	29.9	16.6	94.8		para	30.3	5.01	14.2

insertion into the pore occurs. Fig. S1† shows the chromatograms of ZnJAST4 and ZnJAST1 when using divinylbenzene (as a mixture of *ortho*, *meta*, and *para* isomers) as the analyte. Three peaks were observed with both MOFs, but the peak shapes indicated that the elution orders were different. When chloroform was added to hexane as the mobile phase, the retention of most analytes decreased. Thus, in the case of a halogen-substituted analyte, the halogen bond may contribute to retention by the MOF. However, in the case of nitro-group substitution, the elution orders fluctuate back and forth, that is, inexplicable behavior is observed. With regard to this phenomenon, further study is required.

3.5 Evaluation of retention behavior of polysubstituted benzenes

Table S3† summarizes the values of the retention coefficient, k, of predominantly tri-substituted benzenes and a number of polysubstituted benzenes, for each column. Notably, 1,3,5-tri-halogenated benzenes exhibited minimal retention. This behavior may be attributed to the predominance of halogen bonding in 1,3,5-trihalogenated benzenes, which appears less effective compared to the hydrogen bonding and π stacking that governs retention of dihalogenated benzenes as described in our previous study.[25,27] Besides, the retention of Br-substituted benzenes was greater than that of other halogens. It is proposed that ZnJAST1 should be used specifically to retain bromine-substituted benzenes. With the ZnJAST4 column, the retention coefficient value of each of hexamethylbenzene and hexaphenylbenzene was $k < 0$, which may be influenced by size-exclusion effects.

3.6 Evaluation of the retention behavior of PAHs

Table 3 summarizes the values of the retention coefficient, k, of PAHs with each column. In comparing benzene with the PAHs of naphthalene, anthracene, and naphthacene, all of which consist of linearly fused benzene rings, column retention becomes stronger in line with the increase in the number of π electrons. Comparing analytes having the same number of π electrons, those having bent structures exhibit stronger reten-

Table 3 The retention coefficients of PAHs in the hexane mobile phase

Analyte	ZnJAST4	CuJAST4	ZnJAST1
Benzene	0.84	0.55	0.88
Naphthalene	1.72	1.00	3.75
Acenaphthene	1.08	1.24	3.50
Anthracene	6.09	2.15	5.07
Phenanthrene	5.62	2.65	6.61
Naphthacene	7.76	1.44	42.9
Benz[a]anthracene	8.08	3.30	24.0
Chrysene	3.61	0.82	46.7
Triphenylene	0.09	0.12	13.8
o-Terphenyl	0.02	0.03	0.32
o-Terphenyl	5.09	1.47	0.83
o-Terphenyl	30.3	5.01	14.2
Pyrene	3.10	2.30	11.0
Coronene	0.17	0.48	0.31
Corannulene	0.67	0.38	73.8

tion than those having linear structures. Thus, an additional factor other than insertion into pores, namely polarity of analytes, may affect retention. In particular, corannulene, which exceeds the pore aperture of ZnJAST1, was nonetheless strongly retained. This is likely due to its pronounced dipole moment oriented perpendicular to its curved structure.[28–30] When retention was evaluated in toluene as the mobile phase using the ZnJAST4 and the ZnJAST1 columns, no analytes were retained with the ZnJAST4 column, but triphenylene and corannulene were slightly retained with ZnJAST1. Therefore, it is concluded that the retention in hexane as the mobile phase was affected by π electrons, and certain molecular recognition toward bulky, curved aromatic molecules may likely have occurred.

3.7 Elution behavior of PEGs with etherified termini in the ZnJAST4 column

Fig. 3 shows chromatograms of PEGs with etherified termini at 25 °C, while elution times of each analyte are listed in Table S4.† When the number of terminal alkyl chains in the ether groups is increased, the retention time becomes longer. This suggests that increasing the number of terminal carbons increases affinity between the modified PEG and the MOF. At
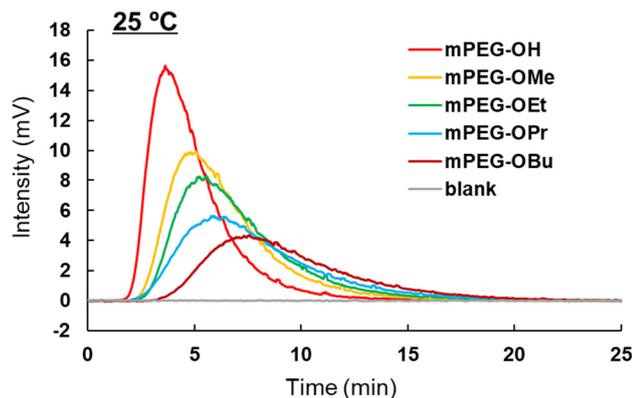
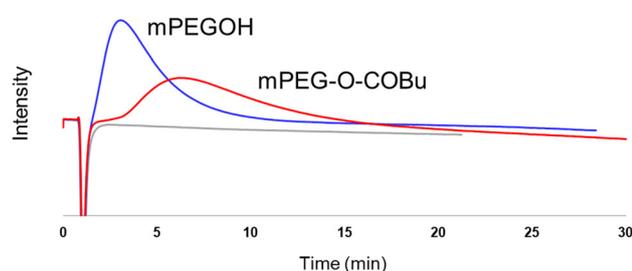**Fig. 3** Chromatograms of single-end type analytes at 25 °C.

Fig. 4 Chromatograms using the ZnJAST4 column of PEGs with esterified termini.

the retention mechanisms involving hydrogen bonding, halogen bonding, π stacking, polarity, and size effects gave rise to complex separation behavior. In the second part, using PEGs with different end groups as samples, the possibility of separation based on terminal polarity was demonstrated. Further investigation of the retention mechanisms may reveal correlations between the MOF structure and molecular recognition, which could enable these MOFs to effectively separate substances such as divinylbenzene and synthetic polymers that are more challenging to resolve.

Author contributions

All authors contributed to and have given approval for the final version of the manuscript. T. Kubo: supervision, project administration, funding acquisition, conceptualization, methodology, writing – original draft, writing – review & editing; K. Matsubara, Y. Watabe, N. Hosono, T. Uemura: conceptualization, methodology; S. K.-Yamada: writing – original draft, writing – review & editing. The authors thank N. Mizutani for her assistance in the preparation of the PEG analytes.

Conflicts of interest

There are no conflicts to declare.

Data availability

Data are available upon request from the authors.

the same time, the retention time is decreased by raising the temperature (Fig. S2†). This may be described in terms of the molecular motion of the PEG intensifying as the temperature is increased, which hampers its interaction with the MOF.

3.8 Elution behavior of PEGs with esterified termini in the ZnJAST4 column

The chromatograms shown in Fig. 4 indicate that the elution time of mPEG-OCOBu is significantly longer than that of mPEG-OH, with retention times of 2.96 min and 6.25 min, respectively. The separation factor, $\alpha_{\text{mPEGOCOBu/mPEGOH}}$ (defined as the ratio of retention factors for mPEG-OCOBu and mPEG-OH), was 2.73 ($t_0 = 1.06$ min), suggesting that esterification of the terminal hydroxyl group increases the analyte's affinity for the ZnJAST4 stationary phase, likely due to reduced polarity and an extended hydrophobic chain length.

Acknowledgements

4. Conclusion

In the first part of this study, MOFs including ZnJAST4, CuJAST4, and ZnJAST1, which have different metallic ions and acidic ligands, were packed into HPLC columns, and benzene derivatives were analyzed. As a result, the retention behavior characteristics of conventional size exclusion chromatography were not observed; however, the gate size of the MOF crystals contributed strongly to molecular recognition. Furthermore,

References

1 M. Kamigaito, T. Ando and M. Sawamoto, *Chem. Rev.*, 2001, **101**, 3689–3746.

2 M. Ouchi, T. Terashima and M. Sawamoto, *Chem. Rev.*, 2009, **109**, 4963–5050.

3 N. Hosono and T. Uemura, *Matter*, 2020, **3**, 652–663.

4 H.-C. Zhou and S. Kitagawa, *Chem. Soc. Rev.*, 2014, **43**, 5415–5418.

5 S. L. James, *Chem. Soc. Rev.*, 2003, **32**, 276–288.

6 A. Jenabi, M. A. F. Maghsoudi, M. Daghigh and R. M. Aghdam, *J. Drug Delivery Sci. Technol.*, 2024, **94**, 105489.

7 H. Yuan, N. Li, W. Fan, H. Cai and D. Zhao, *Adv. Sci.*, 2022, **9**, 2104374.

8 A. J. Rieth, A. M. Wright and M. Dincă, *Nat. Rev. Mater.*, 2019, **4**, 708–725.

9 Z. Zhu, H. Tsai, S. T. Parker, J.-H. Lee, Y. Yabuuchi, H. Z. Jiang, Y. Wang, S. Xiong, A. C. Forse and B. Dinakar, *J. Am. Chem. Soc.*, 2024, **146**, 6072–6083.

10 Y. Yao, X. Wei, H. Zhou, K. Wei, B. Kui, F. Wu, L. Chen, W. Wang, F. Dai and P. Gao, *ACS Catal.*, 2024, **14**, 16205–16213.

11 Y.-B. Huang, J. Liang, X.-S. Wang and R. Cao, *Chem. Soc. Rev.*, 2017, **46**, 126–157.

12 M. Hu, Y. Ju, K. Liang, T. Suma, J. Cui and F. Caruso, *Adv. Funct. Mater.*, 2016, **26**, 5827–5834.

13 S. Wu, Y. Lin, J. Liu, W. Shi, G. Yang and P. Cheng, *Adv. Funct. Mater.*, 2018, **28**, 1707169.

14 S. Wu, H. Min, W. Shi and P. Cheng, *Adv. Mater.*, 2020, **32**, 1805871.

15 B. Mohan, M. B. Asif and A. J. Pombeiro, *Small*, 2025, **21**, 2406222.

16 B. Mohan, G. Singh, A. Chauhan, A. J. Pombeiro and P. Ren, *J. Hazard. Mater.*, 2023, **453**, 131324.

17 N. Hosono and T. Uemura, *Acc. Chem. Res.*, 2021, **54**, 3593–3603.

18 N. Mizutani, N. Hosono, B. Le Ouay, T. Kitao, R. Matsuura, T. Kubo and T. Uemura, *J. Am. Chem. Soc.*, 2020, **142**, 3701–3705.

19 B. Le Ouay, C. Watanabe, S. Mochizuki, M. Takayanagi, M. Nagaoka, T. Kitao and T. Uemura, *Nat. Commun.*, 2018, **9**, 3635.

20 T. Sawayama, Y. Wang, T. Watanabe, M. Takayanagi, T. Yamamoto, N. Hosono and T. Uemura, *Angew. Chem., Int. Ed.*, 2021, **60**, 11830–11834.

21 K. Kioka, N. Mizutani, N. Hosono and T. Uemura, *ACS Nano*, 2022, **16**, 6771–6780.

22 M. Ding, L. Yang, J. Zeng, X. Yan and Q. Wang, *Anal. Chem.*, 2020, **92**, 15757–15765.

23 A. A. Kotova, D. Thiebaut, J. Vial, A. Tissot and C. Serre, *Coord. Chem. Rev.*, 2022, **455**, 214364.

24 (*a*) H. Chun, D. N. Dybtsev, H. Kim and K. Kim, *Chem. Eur. J.*, 2005, **11**, 3521–3529; (*b*) T. Uemura, Y. Ono, K. Kitagawa and S. Kitagawa, *Macromolecules*, 2008, **41**, 87–94; (*c*) D. N. Dybtsev, H. Chun and K. Kim, *Angew. Chem., Int. Ed.*, 2004, **43**, 5033–5036.

25 E. Kanao, T. Morinaga, T. Kubo, T. Naito, T. Matsumoto, T. Sano, H. Maki, M. Yan and K. Otsuka, *Chem. Sci.*, 2020, **11**, 409–418.

26 L. Hamon, I. Andrusenko, A. Borzì, M. Stiefel, S. Carl, R. Frison, A. Cervellino, M. Gemmi, G. Santiso-Quinones and E. Hovestreydt, *Mater. Adv.*, 2022, **3**, 6869–6877.

27 E. Kanao, H. Osaki, T. Tanigawa, H. Takaya, T. Sano, J. Adachi, K. Otsuka, Y. Ishihama and T. Kubo, *Anal. Chem.*, 2023, **95**, 9304–9313.

28 T. Kubo, E. Kanao, T. Matsumoto, T. Naito, T. Sano, M. Yan and K. Otsuka, *ChemistrySelect*, 2016, **1**, 5900–5904.

29 T. Kubo, Y. Murakami, Y. Tominaga, T. Naito, K. Sueyoshi, M. Yan and K. Otsuka, *J. Chromatogr. A*, 2014, **1323**, 174–178.

30 T. Kubo, Y. Murakami, M. Tsuzuki, H. Kobayashi, T. Naito, T. Sano, M. Yan and K. Otsuka, *Chem. – Eur. J.*, 2015, **21**, 18095–18098.